

Structural phase transformation in InSb: A molecular dynamics simulation

S. C. Costa, P. S. Pizani, and J. P. Rino*

Departamento de Física, Universidade Federal de São Carlos, Caixa Postal 676, 13565-905, São Carlos, SP, Brazil

(Received 28 June 2002; published 27 December 2002)

An isoenthalpic-isobaric molecular dynamics simulation was used to study the structural properties of crystalline InSb, based on an effective interaction potential. The interaction potential consists of an effective pair potential which takes into account atomic-size effects and charge-charge, charge-dipole, dipole-dipole, and three-body interactions, the last needed to describe bond bending and bond stretching. The system consists of 1000 particles (500 In and 500 Sb) initially in a cubic box of side $L=32.397$ Å. The simulation of the pressure-induced structural transformation was done at fixed temperature, with the external pressure increasing in steps of 0.2 GPa up to 6.0 GPa. The phase transformation from fourfold-coordinated zinc-blende to sixfold-coordinated orthorhombic structure is successfully reproduced at the correct experimental value of ~ 3 GPa. Pair distribution function, coordination number, volume change, and bond angle distributions are presented and compared with experimental available data.

DOI: 10.1103/PhysRevB.66.214111

PACS number(s): 61.20.Ja, 61.43.Bn, 61.43.Dq, 62.50.+p

I. INTRODUCTION

The study of the influence of pressure and temperature on the properties of materials is very interesting since it can furnish information about phase transitions. In particular, experiments in semiconductors under high-pressure conditions have been done since the 1960s.¹ Many of the III-V semiconductors undergo a semiconductor-to-metal transition under high pressure. Among them, InSb is one that presents the lowest-pressure-induced structural transformation. In the 1970s x-ray diffraction was used to study the structural transformation in indium antimonide up to 2.8 GPa.²⁻⁴ In the next decade Vanderborgh *et al.*, using energy-dispersive x-ray diffraction, studied this system up to 66 GPa.⁵ Most of the experimental results indicated that its cubic structure, at room temperature, transforms either to a mixture of $P2$ (tetragonal β -tin structure) and $P3$ (orthorhombic) phases at ~ 2.1 GPa, followed by a single-phase $P3$ and before crystallizing in the $P4$ orthorhombic phase, or directly transform to $P4$ at ~ 3.0 GPa. Recently, Nelmes *et al.*⁶ reexamined, by using an angle-dispersive powder-diffraction technique on a synchrotron source, the structural transformation in InSb up to 5 GPa, showing that the established pressure-temperature (P - T) phase diagram was incorrect. Finally, further experiments⁷ have shown that the phase $P2$, in fact, does not exist, but is an orthorhombic phase. On the other hand, from the theoretical point of view, there are some pseudopotential and first-principle density functional total energy calculations studies of this material. However, these calculations were performed at a structural ground-state configuration.⁸⁻¹⁰

In this paper we report the results of an isoenthalpic-isobaric molecular dynamics (MD) simulation of the pressure-induced structural transformation in InSb, up to 6 GPa, based on an effective two- and three-body interaction potential.

II. INTERACTION POTENTIAL AND MOLECULAR DYNAMICS CALCULATION

The central core of a molecular dynamics simulation is the choice of the interatomic potential, which determines the

failure or success of a simulation. There are tens of empirical interaction potentials which have been used to describe elemental semiconductors, metals, III-V and II-VI semiconductors, and more complex systems.^{11,12} Among all these empirical interaction potentials we choose the interaction potential proposed by Shimojo *et al.*,¹³ which has been used to describe several different systems.¹⁴⁻¹⁸ The total interaction potential consists of effective two-body and three-body terms

$$\Phi = \sum_{i<j} V^{(2)}(r_{ij}) + \sum_{i<j<k} V^{(3)}(r_{ij}, r_{ik}). \quad (1)$$

The two-body interaction reads as

$$V(r) = \frac{H_{\alpha\beta}}{r^{\eta_{\alpha\beta}}} + \frac{Z_{\alpha\beta}e^{-r/\lambda}}{r} - \frac{D_{\alpha\beta}e^{-r/\xi}}{2r^4} - \frac{W_{\alpha\beta}}{r^6}, \quad (2)$$

where the first term takes into account steric repulsion (with parameters $H_{\alpha\beta}$ and $\eta_{\alpha\beta}$), the second term is the Coulomb interaction due to charge transfer between ions, the third term is the charge-dipole interaction due to the large electronic polarizability of anions, and the last one is the van der Waals (dipole-dipole) type interaction. The three-body interaction, necessary to take into account covalent effects, is a modified Stillinger-Weber¹¹ type potential given by

$$\begin{aligned} V^{(3)}(r_{ij}r_{ik}) = & B_{ijk} \exp \left[\frac{\gamma}{r_{ij}-r_0} + \frac{\gamma}{r_{ik}-r_0} \right] \\ & \times \frac{(\cos \theta_{ijk} - \langle \cos \theta_{ijk} \rangle)^2}{1 + C(\cos \theta_{ijk} - \langle \cos \theta_{ijk} \rangle)^2} \Theta(r_0 - r_{ij}) \\ & \times \Theta(r_0 - r_{ik}), \end{aligned} \quad (3)$$

where B_{ijk} is the strength of the interaction, $\Theta(r_0 - r_{ij})\Theta(r_0 - r_{ik})$ are step functions, $\langle \cos \theta_{ijk} \rangle$ is a constant, and θ_{ijk} is the angle between r_{ij} and r_{ik} . The screenings in the Coulomb and in the charge-dipole interactions are introduced in order to avoid the long-range calculations in these interactions. The range of screening parameters was fixed in $\lambda = 5.0$ Å and $\xi = 3.75$ Å, and the two-body potential is trun-

TABLE I. Experimental (Refs. 23 and 24) and molecular dynamics values of the lattice parameter, elastic constants, bulk modulus, cohesive energy, and melting temperature for InSb.

	Experiment	Molecular dynamics
Lattice parameter (Å)	6.4794	6.4794
Elastic constants (GPa)		
C_{11}	65.76	65.7
C_{12}	35.65	35.6
C_{44}	29.83	25.2
Bulk modulus	45.73	45.63
Cohesive energy (eV/N)	2.80	2.795
Melting temperature (K)	800	1300±50

cated at $r_c = 7.5 \text{ \AA}$. The interaction potential for $r < r_c$ is shifted as usual,^{19,20} in order to have the value and its first derivative continuous at the cutoff length. From other simulations using this type of potential^{13,14,21} we took the exponents η_{InIn} , η_{InSb} , and η_{SbSb} to be 7, 9, and 7, respectively. The remaining constants were determined from the cohesive energy, elastic constant, bulk modulus, and melting temperature.

The molecular dynamics simulations were performed in the HPN ensemble (Parrinello-Rahman, which allows changes of the size and shape of the simulation box),²² in a system consisting of 1000 particles (500 In + 500 Sb). Initially the particles were arranged in a cubic zinc-blende structure at actual density, with zero external pressure. The system was then heated until temperature reaches 900 K, when we start applying external pressure in a rate of 0.2 GPa per 50 000 time steps, up to 6.0 GPa. For all applied pressures the temperature was kept constant at that value by scaling the velocity of particles every 100 time steps.

For each applied external pressure, the system was thermalized by 50 000 time steps of 2.5 fs, and the phase space has been examined in order to provide two-body structural correlations through pair distribution function and coordination numbers, as well as three-body correlations through bond-angle distributions. It is known that the time scale for volume and shear fluctuations in the simulation ought to be on the order of a few vibrational periods; hence, they are by definition orders of magnitude smaller than experimental (seconds). Nevertheless, the phase transition may well occur very rapidly, as we discuss below. To determine the melting temperature, starting from the cubic zinc-blende structure, the system was heated at constant zero external pressure up to 1500 K. For each temperature the system was allowed to relax for 50 000 time steps.

III. RESULTS AND DISCUSSION

The experimental values of the physical constants shown in the Table I were used to calibrate the interaction potential, that is, to adjust the parameters used in Eqs. (2) and (3). Once the results from the simulations reproduce well these values, the potential parameters are fixed to simulate all other properties. The values of the potential parameters for InSb are also displayed in Table II. At zero pressure and zero

TABLE II. Parameters used in the interaction potential for InSb. λ, ξ, r_c in angstroms and the energies in erg.

	In-In	In-Sb	Sb-Sb
$H_{\alpha\beta}$	5.5933×10^{-10}	2.4105×10^{-8}	1.2022×10^{-8}
$Z_{\alpha\beta}$	$0.86825e^2$	$-0.86825e^2$	$0.86825e^2$
$D_{\alpha\beta}$	0	$2.60476e^2$	$5.20951e^2$
$W_{\alpha\beta}$	0	14.539×10^{-10}	0
$\eta_{\alpha\beta}$	7	9	7
$\lambda = 5.0$	$\xi = 3.75$	$r_{cut} = 7.5$	$e = \text{electron charge}$

degree kelvin the ground-state zinc-blende structure is stable.

Figure 1 shows the total energy per particle as a function of temperature. The discontinuity in energy around $1300 \pm 50 \text{ K}$ characterizes the calculated melting transition. The highest value of the melting temperature obtained from the MD simulation could be attributed to the periodic boundary conditions imposed on the system.

To simulate the pressure effects on InSb, for each applied pressure, after the system has been very well thermalized, averages were taken over additional 20 000 time steps. In this study the temperature of the system was set to be 900 K. In Fig. 2 we show, at 3.0 GPa, the time evolution of the MD cell vectors. Up to 2.8 GPa the MD cell is cubic, and the system remains zinc-blende four-fold coordinated. Around 3.0 GPa the structural transformation occurs, as can be seen by the changes in the MD lengths L_1 , L_2 , and L_3 . This transformation was also confirmed by the changes in the bond length, In-Sb and first neighbors Sb-Sb and In-In, as a function of pressure. The increase in In-Sb bond length is followed by the increase of coordination number, as displayed in Fig. 3, which clearly confirms the structural transformation from a fourfold- to sixfold-coordinated orthorhombic structure under pressure. Similar results have been obtained for other materials such as GaAs and SiC, using the

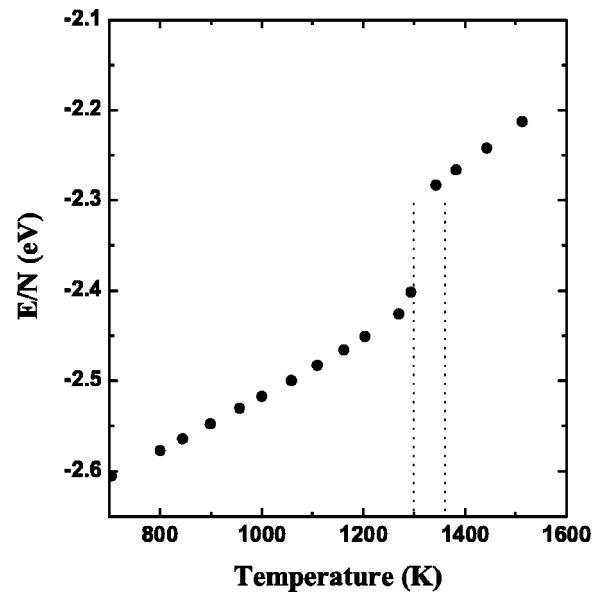


FIG. 1. Energy per particle as a function of the temperature. The dotted lines at about 1300 K indicate the melting temperature.

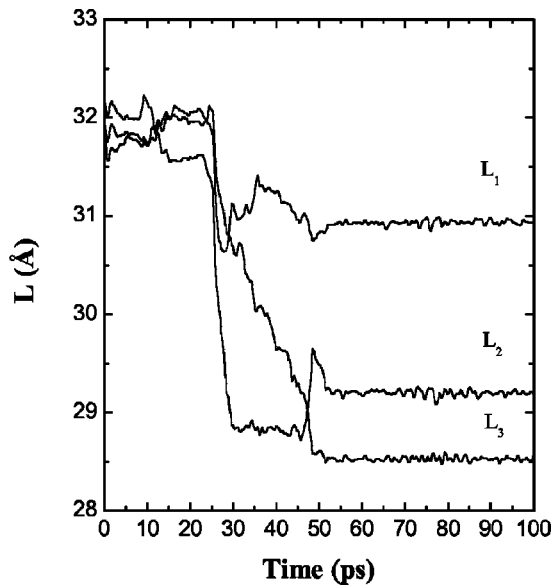


FIG. 2. The time evolution of the molecular dynamics cell vectors, showing the structural phase transition from cubic to orthorhombic.

same functional form for the interaction potential.

A comparison of experimental and MD results for the volume-pressure relationship for InSb is shown in Fig. 4. An excellent agreement of the MD results, in a wide range of pressure, can be observed. The volume reduction due to compression, just before the transition, at 2.8 GPa is $0.925V_0$ (V_0 is the volume at ambient pressure), which agrees very well with experimental results of $0.93V_0$. The volume reduction due to the structural transformation was found to be 19.7%, which also agrees very well with the experimental result reported by Nelmes *et al.*,⁶ 19.5%, and Yu *et al.*,⁴

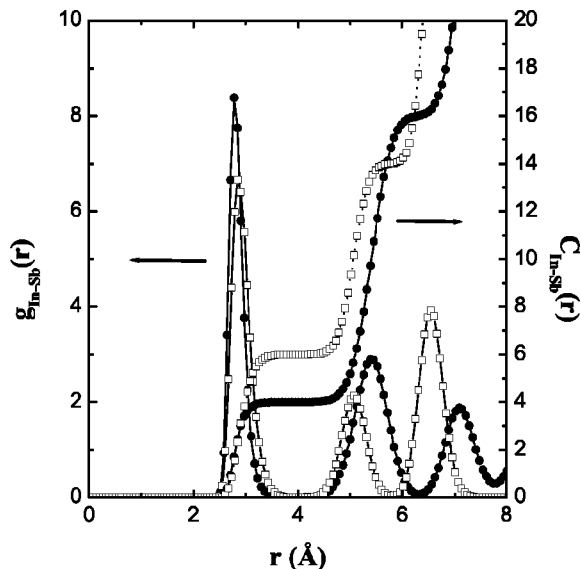


FIG. 3. The In-Sb pair distribution function (left) and coordination number (right) around In and Sb atoms for pressures just before and after the structural transformation. Solid circles at 2.8 GPa and open squares at 3.0 GPa.

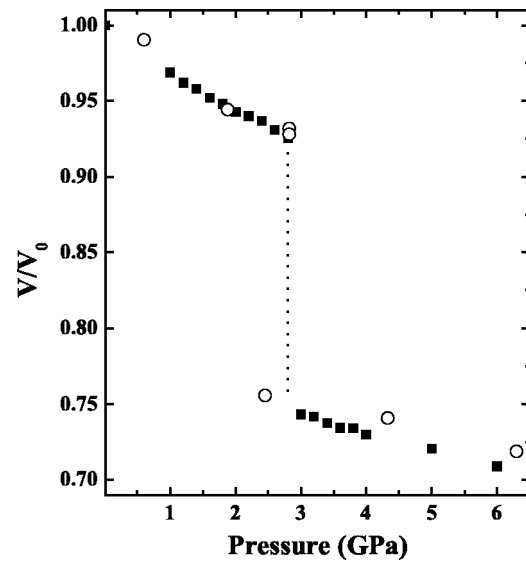


FIG. 4. Changes of the reduced volume as a function of the hydrostatic pressure. Open circles from Ref. 5 and solid squares from the molecular dynamics simulation. The dotted line indicates the structural phase transition.

19.3%, but larger than that reported by Vanderborgh *et al.*⁵ 17.1%.

The three-body correlations were analyzed through the bond-angle distribution. Figure 5 displays the Sb-In-Sb bond-angle distribution at 2.8 and 3.0 GPa. At pressures below the structural transition the bond angle is peaked at 109° (internal tetrahedral angle), and at the transition this angle moves to 90° and 180° , characteristic of an orthorhombic phase. These results clearly demonstrate that the structural transformation from a tetrahedrally fourfold-coordinated structure goes to an octahedrally sixfold-coordinated structure under pressure.

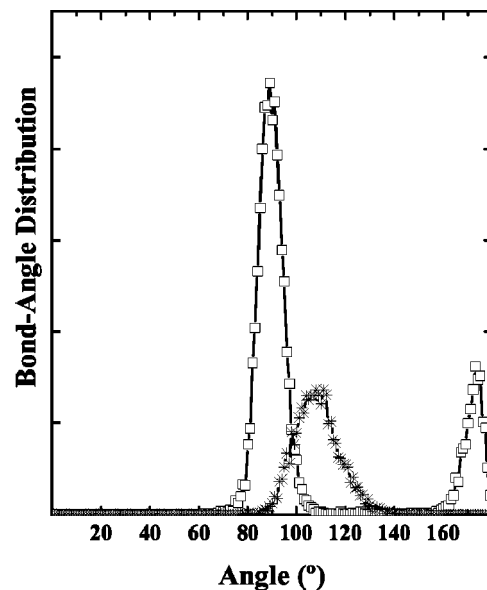


FIG. 5. Sb-In-Sb bond angle at pressures just before and after the structural transformation. Open squares at 2.8 GPa and stars at 3.0 GPa.

IV. CONCLUSIONS

In conclusion, we have performed a Parrinello-Rahman molecular dynamics simulations for the pressure-induced structural transformation in InSb using the effective potential which takes into account two- and three-body interactions. The zinc-blende to orthorhombic structural transformation is very well described, in excellent agreement with experimental observation. The calculated volume changes, before and after transformation, are also in excellent agreement with those observed in experiments. Furthermore, structural parameters such as bond length and coordination number are

correctly reproduced. This potential can be than used to simulate and preview several structural and dynamics properties of InSb as a function of temperature and pressure, including conditions not yet realizable experimentally.

ACKNOWLEDGMENT

This work was partially supported by Fundação de Amparo à Pesquisa do Estado de São Paulo—FAPESP and Conselho Nacional de Desenvolvimento Científico e Tecnológico—CNPq.

*Electronic address: djpr@df.ufscar.br

¹A.J. Darnell and W.F. Libby, Phys. Rev. **135**, A1453 (1964).

²K. Asaumi, O. Shimomura, and S. Minomura, J. Phys. Soc. Jpn. **41**, 1630 (1976).

³O. Shimomura, K. Asaumi, N. Sakay, and S. Minomura, Philos. Mag. **34**, 839 (1976).

⁴S.C. Yu, I.L. Spain, and E.F. Skelton, Solid State Commun. **25**, 49 (1978).

⁵C.A. Vanderborgh, Y.K. Vohra, and A.L. Ruoff, Phys. Rev. B **40**, 12 450 (1989).

⁶R.J. Nelmes, M.I. McMahon, P.D. Hatton, J. Crain, and R.O. Piltz, Phys. Rev. B **47**, 35 (1993).

⁷R.J. Nelmes and M.I. McMahon, Phys. Rev. Lett. **77**, 663 (1996).

⁸S.B. Zang and M.L. Cohen, Phys. Rev. B **35**, 7604 (1987).

⁹G.Y. Guo, J. Crain, P. Blaha, and W.M. Temmermen, Phys. Rev. B **47**, 4841 (1993).

¹⁰A.A. Kelsey and G.J. Ackland, J. Phys.: Condens. Matter **12**, 7161 (2000).

¹¹F.H. Stillinger and T.A. Weber, Phys. Rev. B **31**, 5262 (1985).

¹²S. Erkoç, Phys. Rep. **278**, 79 (1997) (in this paper several empirical interaction potentials are discussed).

¹³F. Shimojo, I. Ebbsjo, R.K. Kalia, A. Nakano, J.P. Rino, and P. Vashishta, Phys. Rev. Lett. **84**, 3338 (2000).

¹⁴I. Ebbsjo, R.K. Kalia, A. Nakano, J.P. Rino, and P. Vashishta, J.

Appl. Phys. **87**, 7708 (2000).

¹⁵W. Li, R.K. Kalia, and P. Vashishta, Phys. Rev. Lett. **77**, 2241 (1996).

¹⁶R.K. Kalia, A. Nakano, K. Tsuruta, and P. Vashishta, Phys. Rev. Lett. **78**, 689 (1997).

¹⁷R.K. Kalia, A. Nakano, A. Omeltchenko, K. Tsuruta, and P. Vashishta, Phys. Rev. Lett. **78**, 2144 (1997).

¹⁸P. Vashishta *et al.*, in *Amorphous Insulators and Semiconductors*, edited by M.F. Thorpe and M.I. Milkova, Vol. 3 of *NATO Advanced Study Institute, Series 3* (Kluwer, Boston, 1996).

¹⁹M.P. Allen and D.J. Tildesley, *Computer Simulation of Liquids* (Clarendon Press, Oxford, 1997).

²⁰A. Nakano, R.K. Kalia, and P. Vashishta, J. Non-Cryst. Solids **171**, 157 (1994).

²¹J.P. Rino, A. Chatterjee, I. Ebbsjö, R.K. Kalia, A. Nakano, F. Shimojo, and P. Vashishta, Phys. Rev. B **65**, 195206 (2002).

²²M. Parrinello and A. Rahman, Phys. Rev. Lett. **45**, 1196 (1980); J. Appl. Phys. **52**, 7182 (1981).

²³*Numerical Data and Functional Relationships in Science and Technology*, edited by O. Madelung, M. Schulz, and H. Weiss, Landolt-Börnstein, New Series, Group III, Vol. 17a, Pt. 327 (Springer-Verlag, Berlin, 1982).

²⁴W.A. Harrison, *Electronic Structure and the Properties of Solids* (Freeman, San Francisco, 1980).